Meas. Sci. Technol. **20** (2009) 055204 (8pp) doi:10.1088/0957-0233/20/5/055204

Electron optical study of the Venus Express ASPERA-4 Electron Spectrometer (ELS) top-hat electrostatic analyser

Glyn A Collinson[1], D O Kataria[1], Andrew J Coates[1], Sharon M E Tsang[1], Christopher S Arridge[1], Gethyn R Lewis[1], Rudy A Frahm[2], J David Winningham[2] and Stas Barabash[3]

[1] Mullard Space Science Laboratory, Holmbury St Mary, UK
[2] Southwest Research Institute, San Antonio, Texas, USA
[3] Swedish Institute of Space Physics, IRF, Kiruna, Sweden

E-mail: gac@mssl.ucl.ac.uk

Received 24 November 2008, in final form 18 March 2009
Published 17 April 2009
Online at stacks.iop.org/MST/20/055204

Abstract
The performance of the Venus Express (VEX) ASPERA-4 Electron Spectrometer (ELS) is different from the nominal response shown by the ASPERA-3 ELS aboard Mars Express due to machining tolerance. Up to now, the precise mechanism for this was unknown and, therefore, the results of the experimental calibration could not be supported with a theoretical understanding of the fundamental instrument science behind the device. In this study, we show that the difference is due to a misalignment of the inner hemisphere and a widening of the entrance aperture of the instrument. The response of the VEX ELS can be approximated by a combination of a vertical offset of the inner hemisphere of ≈0.6 mm and a lateral offset of less than 0.125 mm, combined with an aperture that is ≈0.54 mm wider than nominal. The resulting *K*-factor, geometric factor, energy resolution and peak elevation are in good agreement with those observed experimentally. Therefore, we now have a good agreement between both laboratory calibration data and computer simulation, giving a firm foundation for future scientific data analysis.

Keywords: ASPERA, Venus Express, space plasma analyser, electrostatic analyser, Electron Spectrometer

1. Introduction

ASPERA-4 (Analyser of Space Plasma and Energetic Atoms) [1] is a suite of four sensors currently in orbit around the planet Venus aboard ESA's Venus Express (VEX) mission [2]. The Electron Spectrometer (ELS) that we study here is a top-hat, hemispherical electrostatic energy analyser [3, 4]. Incident electrons enter the instrument through an aperture and are collimated to within ±2° of the plane of incidence. Electrons then enter a pair of concentric hemispherical electrodes which filter the electrons by energy. When a positive voltage is applied to the inner hemisphere, electrons are deflected into the spectrometer. Particles within the desired energy bandpass $\left(\frac{\Delta E}{E} = 8\%\right)$ are transmitted through and strike a micro-channel plate (MCP) [5]. The readout anode of the MCP is split into 16 pixels to provide azimuthal information. The voltage on the inner hemisphere is stepped to achieve an energy spectrum. Examples of data from Venus are shown in Coates *et al* [6].

The four components that are critical to the mechanical integrity of the instrument are the inner and outer hemispherical electrodes, the ceramic insulator on which they are mounted and the top hat, the position or width of which controls the width of the entrance aperture. For any top-hat plasma analyser, it is important that these components be

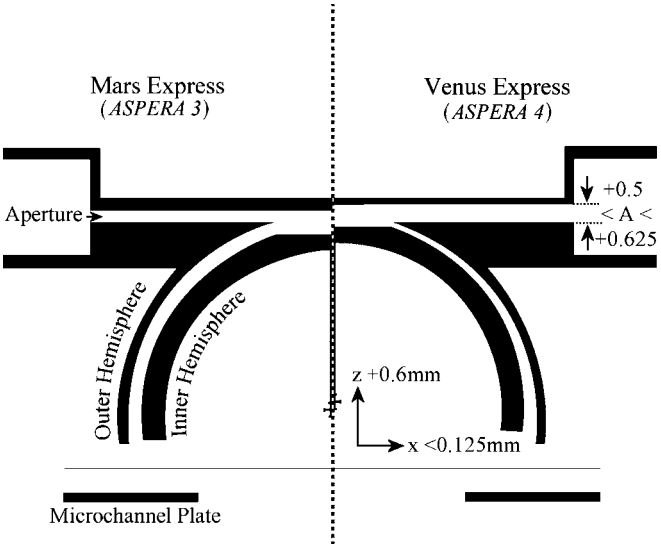

Figure 1. Cross section of ASPERA-ELS (to scale), showing MEX (left) and VEX (right), according to this study.

precisely positioned according to the engineering drawings or the performance of the instrument will be dramatically affected.

The Venus Express ELS under study was never intended to be a flight instrument, but was built as an engineering model as a part of the process of perfecting the manufacturing technique for the ASPERA-3 ELS [7], which is flying on-board ESA's Mars Express (MEX) mission [8]. It was therefore known that the mechanical integrity of the instrument was not as well constrained as the ASPERA-3 ELS, although the exact nature of the misalignments of the components was unknown. Individual components of the deflection system met their tolerance requirements (the radii of the hemispheres were laser measured to within an accuracy of 2.54 μm), but it was discovered that the assembled deflection system exceeded the assembled tolerance specifications (see figure 1). It was not possible to make measurements of the offsets of the assembled components, since all were deep inside the analyser head and inaccessible. Due to funding issues, it was not possible to build a new analyser for Venus Express, and it was decided that the engineering model was to be flown and the response characterized using data from experimental calibration. When the performance of the instrument was characterized using the MSSL plasma calibration facility [9], the response of the instrument was found (as expected) to be dramatically different from the nominal response shown by the flight model ASPERA-3 ELS. The goal of this study is to provide an understanding of the geometry of the analyser in order to explain the instrument's performance, and to provide confidence in the results of the experimental calibration.

The ASPERA ELS sensors are very compact instruments with deflecting surfaces only 1 mm apart. Therefore, with such a diminutive gap, a slight misalignment or a small change in tolerances could greatly affect the instrument parameters. For purposes of UV rejection, the internal components have been blackened using the EBONOL-C process used in the Cluster II PEACE analysers [10]. It was known before launch that the dominant factor in the altered performance is the degree of mechanical alignment and concentricity, which is the main thrust of this study. This misalignment has resulted in dramatic changes in the expected performance of the instrument, specifically in four key instrument parameters (table 1). First is the geometric factor, including efficiencies. Without an accurate determination of the geometric factor, it is impossible to accurately determine particle flux or the distribution function of the particles being measured, from which properties such as density and temperature can be calculated. In this study, the geometric factor was calculated using a modified version of that proposed by Johnstone and co-workers [11] (equation (1)):

$$\text{G.F.} = \frac{eA_F}{I_0 T}\Delta v' \Delta\theta \Delta\varphi' N_{\text{MCP}}\, q, \tag{1}$$

where e is the charge of an electron, A_F is the area of electron acceptance, $\Delta v'$ is velocity step (converted to energy step), $\Delta\theta$ the elevation step between measurements, $\Delta\varphi'$ is the azimuthal step, I_0 is the beam current, T is the beam temperature, N_{MCP} is the number of electrons hitting the MCP, and q is the detector efficiency. For ASPERA-4 ELS, this includes an MCP efficiency of 58% (quoted by the manufacturer) and a grid transparency of 81%.

The second important characteristic of the instrument is the K-factor (also often referred to as the analyser constant). The K-factor (K) is the constant of proportionality between the peak of the accepted energy bandpass of a top-hat electrostatic analyser (E), the charge of the particle (q) and the voltage applied to the inner hemisphere (V), where

$$\frac{E}{q} = KV. \tag{2}$$

Without the K-factor, which is azimuthally dependent for ASPERA-4, it is impossible to determine the energy and hence the velocity of the particles entering the analyser as a function of azimuth. Another important value is the energy resolution. The energy resolution of the detector is defined as the full width half maximum of the energy pass-band (ΔE) divided by the peak of the energy pass-band (E_0), where

$$\text{energy resolution} = \frac{\Delta E}{E_0}. \tag{3}$$

A top-hat electrostatic analyser has a bandpass of elevation acceptance approximating to a Gaussian. The peak of the acceptance bandpass is referred to as the peak elevation

Table 1. Comparing ASPERA-3 and ASPERA-4 calibration results and the results of the simulation.

	MEX lab. [7]	MEX sim.	VEX lab. (mean)	VEX sim. (mean)
K	7.2	6.7	10.66	[a]
$\Delta E/E$	8%	7.8%	8.26%	8.05%
G.F. ($\times 10^{-4}$) cm^{2}sr (eV/eV)	7.5	7.3	1.3	0.9

[a] The experimental K-factor (in which there is good confidence) was used to interpolate the $\frac{\Delta E}{E}$ and G.F.

(el_0). In the ideal case, the peak of the elevation bandpass should be oriented along the axis of the aperture (0°):

$$\text{peak elevation} = el_0. \quad (4)$$

The full width half maximum of the elevation bandpass is referred to as the angular resolution (Δel). The nominal value for the MEX ASPERA-3 ELS is 2.5°:

$$\text{angular resolution} = \Delta el. \quad (5)$$

The calibrated geometric factor, *K*-factor and energy resolution of the ASPERA-4 ELS are different than the nominal response shown by the ASPERA-3 ELS. Before this study, the mechanism for the change in all three characteristics was unexplained and, therefore, the results of the experimental calibration could not be supported with a theoretical understanding of the fundamental ELS sensor performance.

This is the first study to identify the misalignment of components within an already existing top-hat space plasma analyser. This is also the first study to examine the effects of a combined offset of the inner hemisphere and a widened entrance aperture. All previous studies of non-concentric space plasma analysers were performed before construction to determine a minimum standard of machining tolerance required to deliver reasonable instrument performance. These studies can be used to give a first-order approximation of what a reasonable offset of the inner hemisphere would have been for the ASPERA-4 ELS. For example, in the Vilpolla *et al* [12] study of the Cassini IBS instrument [13], machining tolerances of 25 μm were required to deliver a maximum permitted loss of 10% of the transmitted particles with respect to the transmission of an ideal instrument. With a gap between the hemispheres, of 2.5 mm, this is equal to a 1% misalignment of the hemispheres. For the ASPERA ELS, with a gap of 1 mm, this is equivalent to 10 μm. A similar study was undertaken by Woodlife [14], who simulated the effect of machining tolerances on the Cluster PEACE instruments [9]. He found that for a maximum of 1% variation in geometric factor, the machining and assembly tolerances required should also not be more than 1%. The ASPERA-ELS sensors are far more compact than the instruments studied by Vilppola and Woodliffe. Therefore, the nominal engineering tolerances of the final ELS sensor on the MEX mission had to be controlled to a greater degree than for IBS and PEACE.

The challenge of delivering an instrument constructed to such a high degree of accuracy required new techniques to be developed for the final assembly of a top-hat space plasma analyser. The instrument under study was never intended as the final product, but as a part of the development of this manufacturing process. It was therefore known before launch that the mechanical integrity of its components was not as tightly constrained as those for the ASPERA-3 ELS aboard MEX. The uncertainty on the 0.88 mm nominal width of the entrance aperture for the ASPERA-4 (VEX) ELS is ±0.635 mm, the possible variation in lateral offset of the inner hemisphere is ±0.457 mm, and the vertical offset of the inner hemisphere ±0.25 mm. In addition to this, because the instrument was constructed as part of a developmental process (and not intended to be a final flight instrument), it is possible that errors in machining may have further compounded these offsets. The instrument was simulated at highest possible resolution of the simulation at the time (0.125 mm), meaning that the instrument was simulated to a higher degree of accuracy than it was actually constructed.

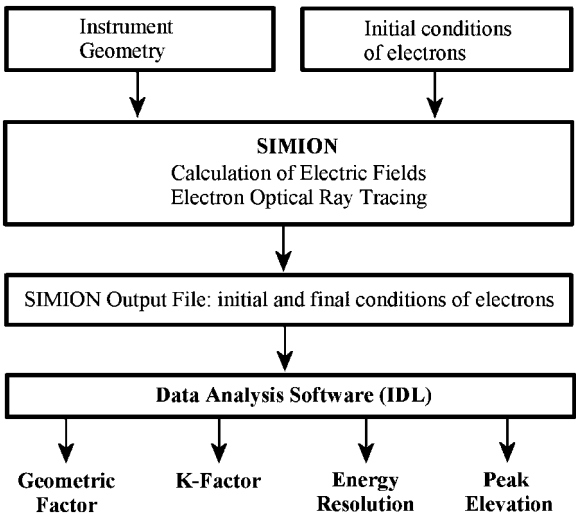

Figure 2. Flowchart showing the simulation method.

In this study, we show first how through computer modelling of the idealized ELS geometry, the performance of the Mars Express ASPERA-3 sensor can be replicated, thus validating the simulation method. Then it is shown how through a combination of a vertical and a horizontal misalignment of the inner hemisphere and a widening of the entrance aperture, the performance of the Venus Express ASPERA-4 ELS can be explained. When the average over all anodes of the experimentally obtained *K*-factor is put into the model, the resulting geometric factor and $\frac{\Delta E}{E_0}$ from the simulation are in good agreement with the calibrated values.

The paper is organized as follows. In section 2, we describe the method of computer simulation and how that method was verified as being accurate. The results of the simulation are outlined in section 3, first introducing a vertical offset of the inner hemisphere, then adding a lateral offset and finally widening the entrance aperture. Finally, the results are discussed in section 4.

2. Simulation method

2.1. Toolkit overview

The simulation method is described in figure 2. Ray-tracing calculations are performed by a commercially available package, SIMION 7.0 and its output is analysed in a series of IDL routines.

SIMION 7.0 is an electrostatic and magnetic field modelling program produced by the Idaho National Engineering and Environmental Laboratory. It models the electrostatic and, where appropriate, magnetic fields generated by each electrode by solving the Laplace equation with boundary conditions, and calculates the forces felt upon charged particles within the simulation space. Simulated

electrons are launched towards the aperture from a two-dimensional grid in discrete steps of elevation and kinetic energy that cover the entire pass-band of values that are accepted by the simulated plasma spectrometer. SIMION calculates the trajectory of each electron through the instrument using standard numerical techniques.

The initial and final kinetic energy, x,y,z coordinates and elevation of each electron are recorded in an ASCII text file. The ASCII output file is analysed in a series of specially written IDL data analysis routines which produce graphical representations of the characteristics of the transmitted particles. The IDL routines also calculate K, G.F., el_0 and $\frac{\Delta E}{E_0}$, and elevation resolution of the sensor.

The results described in this study represent the responses of the ASPERA ELS sensors when a simulated voltage of 150 V is applied to the inner hemisphere. K, G.F., el_0 and $\frac{\Delta E}{E_0}$ are intrinsic response functions and should be independent of the peak of the energy bandpass. When simulations were performed with a range of voltages on the inner hemisphere, it was found that the accepted energy of the incident particles had no effect on the electron optical properties of the instrument.

2.2. Verification of simulation

The Mars Express ASPERA-3 ELS [7] was simulated as a baseline to validate the simulation. The results can be seen in table 1. The 0.125 mm resolution of the simulation means that the dimensions of the simulated electrodes had to be rounded. Since the ASPERA ELS is a very compact design, a few tens of microns can have a small, but noticeable effect on the instrument's performance. This accounts for the small differences (<10%) between the two sets of values and shows that the model can accurately simulate the response of the ASPERA-3 top-hat electrostatic analyser. The geometric factor given in table 1 does not include quantum efficiency factors and is the sum of all 16 anodes. The instrument parameters calculated through 3D simulation are in reasonable agreement (within 10%) with those measured experimentally [7] (see table 1).

2.3. Systematic simulation regime

After simulating the ASPERA-3 ELS as a baseline, the inner hemisphere was systematically offset vertically in steps of 0.125 mm to a maximum value of 0.625 mm, and the simulated response of the instrument recorded. For vertical offsets of 0.5 mm and 0.625 mm, the inner hemisphere was offset laterally around the analyser by 0.125 mm. Due to memory limitations of SIMION 7.0, the step size could not be made any smaller. Simulations were carried out at four positions around the instrument, at 0°, 90°, 180° and 270° (see figure 3). Finally, simulations were repeated for different widths of the entrance aperture, from nominal (0 mm offset) up to +0.625 mm in 0.125 mm steps.

3. Results

3.1. Vertical offset of the inner hemisphere

Figure 4 shows how the K-factor, geometric factor and energy resolution vary when the inner hemisphere is offset vertically.

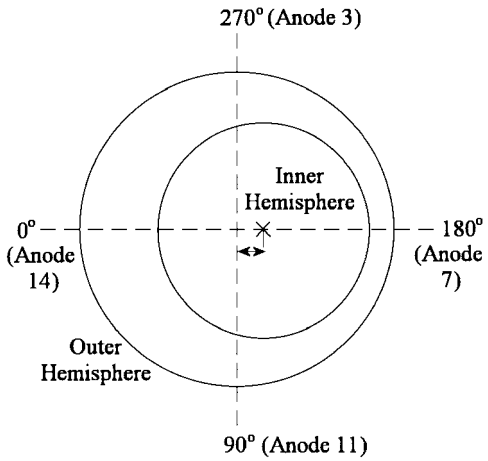

Figure 3. Schematic showing the four simulated lateral misalignments (offset greatly exaggerated).

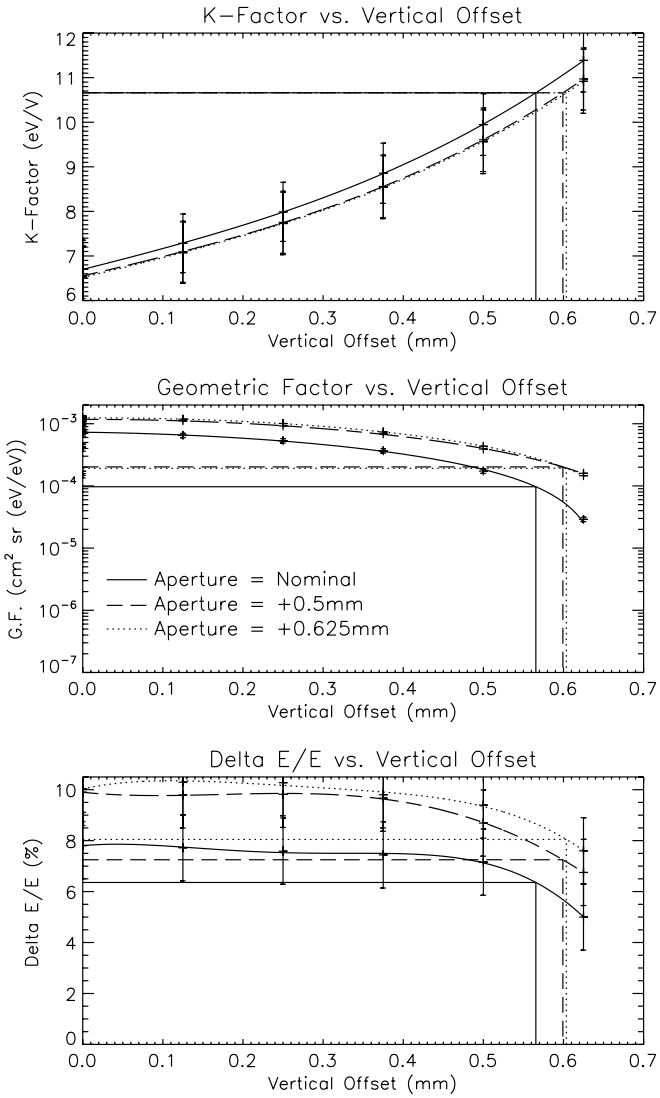

Figure 4. The effect of a vertical offset of the inner hemisphere on G.F., K and $\frac{\Delta E}{E_0}$.

The solid line shows the effect of an increase in the vertical offset of the inner hemisphere alone, and the dashed and dotted

lines show the effect of a combined increase in vertical offset with a +0.5 mm and +0.625 mm wider aperture (described later). The top panel shows the variation of *K*-factor, the middle panel the change in G.F. and the bottom panel the change in energy resolution. As the gap between the two electrodes decreases, for a given voltage on the inner hemisphere, the electric field strength between the electrodes increases. Therefore, less voltage needs to be applied to the inner hemisphere to transmit the incident electron to the MCP, and thus, the *K*-factor increases (see the top panel, figure 4 and equation (2)).

For a nominal instrument, electrons with energies greater than or smaller than the bandpass will impact the inner and outer hemispheres. As the gap between the two hemispheres decreases, the edges of the energy acceptance distribution are blocked, and thus the energy resolution improves and $\frac{\Delta E}{E_0}$ decreases. The reduction of the energy bandpass also decreases the geometric factor (see the middle panel, figure 4). As the gap between the hemispheres decreases, there are fewer paths that electrons can take through the analyser to the MCP. Therefore, the total number of MCP counts decreases, as does the geometric factor.

Many of the characteristics seen in the laboratory calibration of the ASPERA-4 ELS (table 1) therefore, appear to be indicative of a vertical offset of the inner hemisphere. The instrument has an increased *K*-factor, and significantly lower geometric factor as compared to ASPERA-3. The average *K*-factor per anode of the VEX ELS from experimental calibration is 10.66. Interpolation of figure 4 shows how this can be achieved by a 0.57 mm vertical offset of the inner hemisphere. The resulting total G.F. for all 16 anodes is $9.7 \times 10^{-5}\,\mathrm{cm^2 sr(eV/eV)}$ (detector efficiency of 42% not included) and the energy resolution is 6.36%. Both these values are much lower than those measured experimentally (see table 1) suggesting that a vertical offset cannot alone explain the performance of the VEX ELS. Further evidence for this can be found when the performance of the ASPERA-4 is examined at each of its 16 anodes. A vertical offset of the inner hemisphere produces a symmetric instrument response that equally affects the response of all 16 azimuthal sectors. Although a symmetric response was observed in experimental calibration of the MEX ELS, the response of the VEX ELS varies from anode to anode. This further suggests that the performance of the analyser cannot be explained by a vertical offset of the inner hemisphere alone.

3.2. Lateral offset of the inner hemisphere

When a lateral offset of the inner hemisphere is introduced, the response of the instrument varies across the anodes. The panels *A–D* of figure 5 compare the experimental response of the ASPERA-4 ELS to the simulated response of an ELS geometry with a combination of a 0.5 mm and 0.625 mm vertical and a 0.125 mm lateral offset of the inner hemisphere towards anode 7. At the 90° and 270° points (anodes 11 and 3), the gap is largely unchanged and the effects of the lateral offset is small and the instrument parameters are close to those provided by the vertical offset alone (figure 4).

At anode 7, the space between the inner and outer hemispheres is reduced, the electric field strength is increased, and so the *K*-factor also increases (panel *A*, figure 5). Since the experimentally measured *K*-factor is at a maximum at anode 7, this suggests that the inner hemisphere is offset in this direction. At the 0° point (anode 14), the spacing between the hemispheres has increased and so the electric field strength and *K*-factor decrease. The data from the simulated 0.5 mm vertical offset of the inner hemisphere (dotted line, panel *A*, figure 5) give a range of *K*-factors which are too low, whereas the data from the simulated 0.625 mm vertical offset (dashed line, panel *A*, figure 5) give *K*-factors that are too high. The 0.125 mm lateral offset causes a greater variation in simulated *K*-factor response than observed experimentally. Therefore, the actual offset of the inner hemisphere must be less than 0.125 mm. Due to the limitations of resolution of SIMION, it was not possible to determine the precise offset. A lateral offset of 0.125 mm corresponds to a 12% misalignment.

The measured geometric factor response can be seen in panel *B* of figure 5. It is at a minimum at anode 7, where the space between the hemispheres is smallest (180° point), and a maximum at anode 14 where the space between the hemispheres is the widest (0° point). However, the simulated response for a nominal aperture shows the geometric factor varying with a trend that is opposite to the measured response, varying from a maximum at anode 7 to a minimum at anode 14.

Panel *C* of figure 5 shows that the simulated energy resolutions are lower than those measured experimentally. Therefore, although the simulated *K*-factor response is in good agreement with experimental data, G.F., $\frac{\Delta E}{E_0}$ and el_0 are not. This strongly suggests that the performance of the ASPERA-4 ELS cannot be explained through a misalignment of the inner hemisphere alone. To normalize the simulated response of the instrument with that observed, it is necessary to also alter the width of the entrance aperture.

3.3. Widening of the aperture

The combined effect of a vertical and lateral offset of the inner hemisphere plus a widened entrance aperture can be seen in panels *E–H* of figure 5. The *K*-factor (panel *E*) is defined largely by the spacing between the hemispheres and hence, widening of the aperture does not change it significantly. The top panel of figure 4 shows that a ≈+0.6 mm vertical offset of the inner hemisphere is now required to explain the increased *K*-factor of 10.66 for both +0.5 mm and +0.625 mm wider apertures.

The field of view of ELS is approximately ±2°. This value is approximate, since problems with mechanical alignment of the components of the ELS sensor will also affect the geometrical field of view, in particular, since the aperture width has been increased. In panel *D* of figure 5, it can be seen that without an increase in aperture size, the peak elevation lies close to this. However, when the width of the entrance aperture is increased by +0.5 mm (panel *H*), the peak elevation moves back to lie comfortably within the field of view of the instrument. The trend of the experimental data (solid black line) varies in phase with the simulation and now

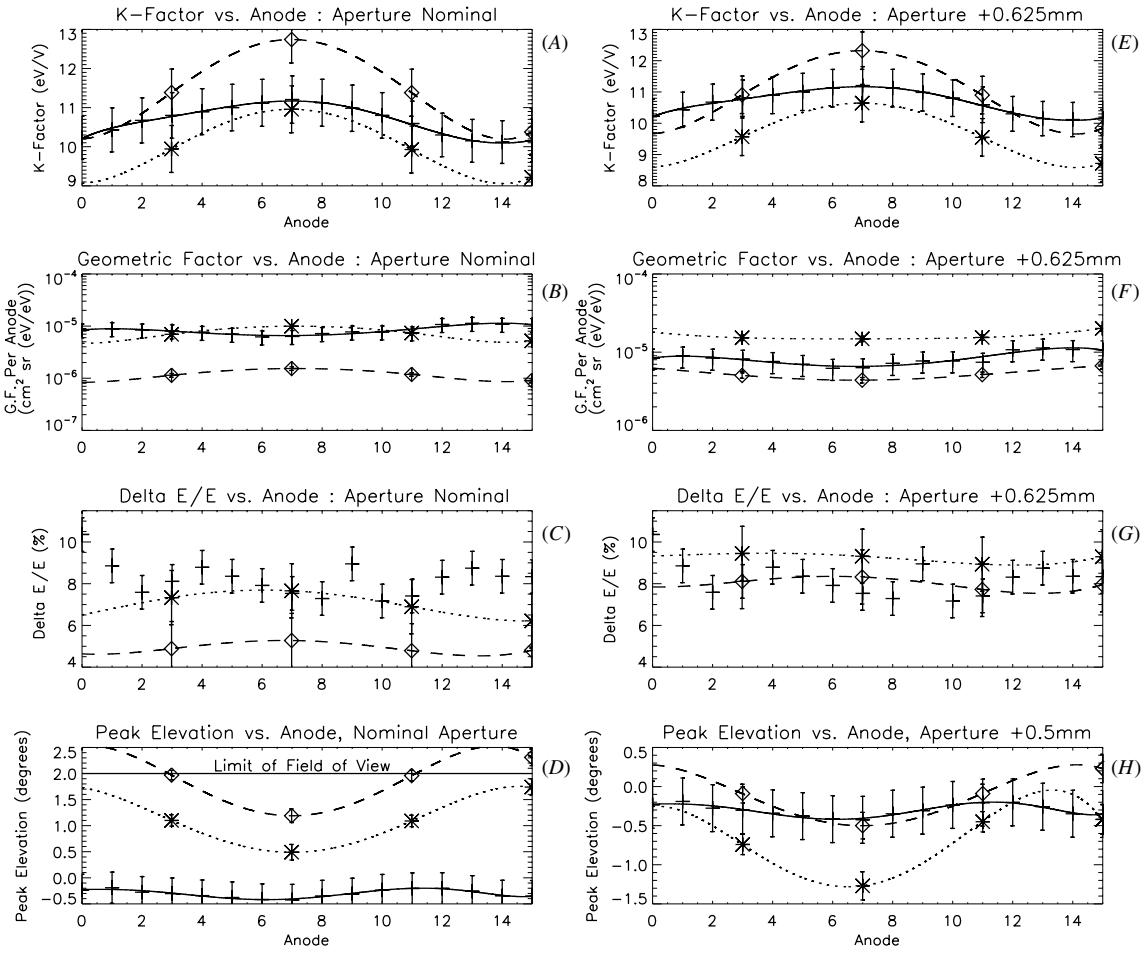

Figure 5. Comparing the experimental response per anode of ASPERA-4 to a simulated combination of a vertical and lateral offset of the inner hemisphere, for both a nominal aperture (panels *A–D*) and an aperture +0.625 mm (panels *E–H*) wider than nominal. (Crosses = 6 keV experimental, diamonds = +0.625 mm vertical +0.125 mm lateral offset, stars = + 0.5 mm vertical +0.125 mm lateral.) (Approximate measurement uncertainties represent our best understanding of error in both simulation and laboratory calibration.)

lies between the +0.5 mm and +0.625 mm inner hemisphere vertical offset curves. This is further evidence that the vertical offset of the inner hemisphere of the VEX ASPERA-4 ELS lies between these values, and the aperture has been widened. Like the *K*-factor response, the variation of the simulated response over the anodes is greater than observed experimentally, which reinforces the theory that the actual lateral offset is less than +0.125 mm.

The simulated energy resolution $\frac{\Delta E}{E_0}$ response (panel *G*, figure 5), is now also in better agreement with the results of the experimental data when the aperture is widened between +0.5 mm and +0.625 mm.

Figure 6 shows a plot at the estimated vertical offset of the inner hemisphere (+0.6 mm) of increase in aperture width versus the peak of the elevation acceptance distribution, el_0. From this it can be shown that the mean experimental value of el_0 (-0.3°) can be used to interpolate an estimated actual offset of ≈+0.54 mm.

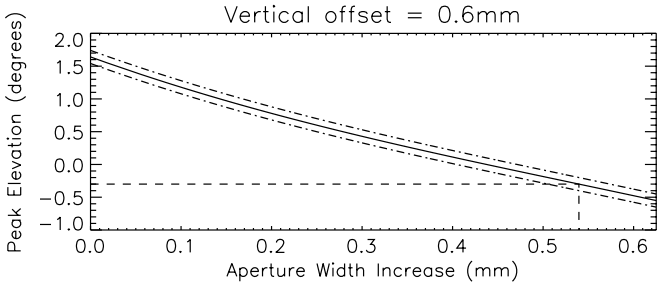

Figure 6. Peak elevation versus increase in aperture width, at an interpolated inner hemisphere vertical offset of +0.6 mm.

4. Discussion

When the idealized (MEX) geometry was simulated, the *K*-factor, G.F. and $\frac{\Delta E}{E_0}$ were in good agreement with the established values, measured previously through laboratory calibration and an independent computer simulation. This both confirms the accepted response of the MEX ELS and validates the method of simulation.

The only misalignment that can explain the dramatic overall increase in *K*-factor from 7.2 (MEX) to 10.66 (VEX average) is for the inner hemisphere of ELS to be vertically offset from the nominal position. An interpolation of *K*-factor versus vertical offset of the inner hemisphere (top panel, figure 4) gives an estimated offset of +0.57 mm (solid black

line). However, when the widening of the aperture is taken into account, this value must be revised. It is shown that there is little difference between the *K*-factor versus offset curves for a widened aperture of either +0.5 mm (dashed line) or +0.625mm (dotted line). Therefore, the estimated vertical offset of the VEX ASPERA-ELS inner hemisphere is ≈0.6 mm. The errors, determined by the 0.125 mm resolution of the simulation are (−0.1 mm, +0.25 mm).

A lateral offset of the inner hemisphere towards anode 7 explains the observed variation in *K*-factor (maximum 11.2 at anode 7, minumum 10.1 at anode 14). This is the same trend as observed by Vilppola [12] and Woodliffe [14]. Because of the limited resolution of the simulation, it was not possible to determine an exact value, although it must be less than 0.125 mm.

The unexpected variation of the simulated G.F. for a nominal aperture (panel *A*, figure 5) is explained through examination of el_0, the peak of the elevation acceptance band-pass (panel *D*, figure 5). The vertical offset of the inner hemisphere has increased the electric field strength in the entrance region, increasing the average peak of the elevation band-pass to ≈2°. Since electrons striking anode 14 pass through this region of increased electric field strength, the peak acceptance angle (el_0) is increased to beyond the approximate ±2° field of view of the instrument (dashed line in panel *D*, figure 5). Therefore, even though the spacing between the hemispheres is larger at anode 14, fewer electrons are accepted and the G.F. is decreased.

Subsequently, the same set of misalignments of the inner hemisphere were then simulated in combination with several different widths of entrance aperture. It was found that a widened aperture with a simultaneous misalignment of the inner hemisphere is the only possible way to explain the experimental response of the ASPERA-4 ELS in *K*-factor, G.F., $\frac{\Delta E}{E_0}$ and el_0. It has been estimated that the width of the entrance aperture is ≈+0.54 mm wider than nominal. The errors, determined by the 0.125 mm resolution of the simulation are (−0.04 mm, +0.085 mm). Since the gap between the inner and outer hemispheres is 1 mm, this vertical offset represents a ≈60% misalignment. These variations are all feasible within a combination of the manufacturing tolerances listed on the original engineering drawings, although they do represent the extremes.

These estimated offsets can be further re-enforced by interpolation of figure 4. From the middle panel of figure 4, it can be shown that a vertical offset of the inner hemisphere of 0.6 mm yields a purely geometric G.F. of 2×10^{-4} cm^{2}sr(eV/eV). When the quantum efficiency of the MCP and grid transparencies are taken into account, this gives an adjusted average G.F. of 0.9×10^{-4} $(+1.2 - 0.9)$ cm^{2}sr (eV/eV) (errors are determined by the resolution of the simulation). This is in good agreement with the average value measured experimentally of 1.3×10^{-4} cm^{2}sr (eV/eV). Furthermore, a +0.6 mm vertical offset of the inner hemisphere yields an energy resolution of 8.05% $(+1.1 - 0.9)$% (bottom panel, figure 4), also in good agreement to that measured experimentally of 8.26% (see table 1).

The solution outlined is unique, since after a systematic study of all possible misalignments of internal components, only one combination explained the experimentally measured response of all four instrument parameters. For example, the widening of the aperture has very little effect on the *K*-factor, so although the response of the G.F. and energy resolution might be replicated, the *K*-factor would no longer match the calibration results. Increasing the radius of the inner hemisphere will increase the *K*-factor, but dramatically reduce the energy resolution. Since the energy resolution measured is actually higher than for the MEX ELS, this cannot be the case.

The widening of the aperture and the lateral offset of the inner hemisphere can be explained through the random accumulation of machining tolerances during construction. However, it may be that the vertical offset of the inner hemisphere is at least in part due to incorrect manufacture or relative positioning. When the MEX flight instrument was constructed, the manufacturing technique had been perfected, and the sources of inaccuracies that arose in the construction of the engineering model had been addressed.

5. Conclusions

During construction, the combination of machining tolerances led to the geometry of the ASPERA-3 (MEX) ELS flight spare being very different than the nominal design, resulting in a dramatic change in the performance of the instrument. Whilst the construction method was perfected for the ASPERA-3 ELS flight model, the precise nature of the misalignment during assembly of the flight spare was not determined before this was re-designated as the ASPERA-4 ELS, and then flown aboard the Venus Express spacecraft. Although a thorough laboratory calibration was performed before launch, the results were not at that time backed up by computer simulation.

Through a systematic set of computer simulations, we have found that the only way that the performance of the ASPERA-4 ELS could be replicated is through a combination of a misalignment of the inner hemisphere and a widening of the entrance aperture (see figure 1). The ≈ + 0.6 mm vertical component of the inner hemisphere offset represented ≈60% of the gap between the hemispheres, and the <0.125 mm lateral component was less than 12% of the gap. The width of the aperture is estimated to be ≈+0.54 mm (61%) wider than nominal. This solution is not only possible within the listed manufacturing tolerances, but is also unique, since no other combination of offsets replicated the response of the instrument in *K*-factor, geometric factor, energy resolution and peak elevation. Therefore, there now exists an estimation of the offsets of the components within ELS and a good understanding of how these offsets have affected the trends of the features observed in the laboratory calibration. This gives a firm foundation for future scientific data analysis using the instrument performance characterized in laboratory calibration.

Acknowledgment

G Collinson is supported by UK STFC studentship funding.

References

[1] Barabash S *et al* 2007 The analyser of space plasmas and energetic atoms (ASPERA-4) for the venus express mission *Planet. Space Sci.* **55** 1772–92

[2] Svedhem H *et al* 2007 Venus express—the first european mission to venus *Planet. Space Sci.* **55** 1636–52

[3] Sablik M J, Golimowski D, Sharber J R and Winningham J D 1988 Computer simulation of a 360° field of view 'top-hat' electrostatic analyzer *Rev. Sci. Instrum.* **59** 146–55

[4] Carlson C W, Curtis D W, Paschmann G and Michel W 1982 An instrument for rapidly measuring plasma distribution functions with high resolution *Adv. Space Res.* **2** 67–70

[5] Adams J and Manley B W 1966 *IEEE Trans. Nucl. Sci.* **NS-13** 88

[6] Coates A J *et al* 2008 Ionospheric photoelectrons at venus: initial observations by ASPERA-4 ELS *Planet. Space Sci.* **56** 802–6

[7] Barabash S *et al* 2006 The analyzer of space plasmas and energetic atoms (ASPERA-3) for the mars express mission *Space Sci. Rev.* **126** 113–64

[8] Chicarro A, Martin P and Trautner R 2004 *The Mars Express Mission: An Overview* (ESA Special Publication 1240) ed A Wilson (Noordwijk: ESA) pp 3–13

[9] Johnstone A D *et al* 1993 *PEACE: a Plasma Electron and Current Experiment* (ESA Special Publication 1159) ed W R Burke (Noordwijk: ESA) p 163

[10] Alsop C, Free S and Scott L 1998 UV rejection design and performance of the PEACE electrostatic analyzers *Geophys. Monogr.* **102** 246–74

[11] Johnstone A D *et al* 1987 The Giotto three-dimensional positive ion analyser *J. Phys. E: Sci. Instrum.* **20** 795–805

[12] Vilppola J H, Keisala J T, Tanskanen P J and Huomo H 1993 Optimization of hemispherical electrostatic analyzer manufacturing with respect to resolution requirements *Rev. Sci. Instrum.* **64** 2190–4

[13] Young D T *et al* 2004 Cassini plasma spectrometer investigation *Space Sci. Rev.* **114** 1–4

[14] Woodliffe R D 1991 Design of space borne plasma analysers by computer simulation *PhD Thesis* Mullard Space Science Laboratory, Department of Physics and Astronomy, University College London